

Real-Time Shim Correction during Functional MRI Using a Volumetric Navigator

A Alhamud¹, Paul Taylor^{1,2}, Jia Fan¹, Ernesta Meintjes¹, and André J.W. van der Kouwe³

¹Human Biology, MRC/UCT Medical Imaging Research Unit, University of Cape Town, Cape Town, Western Cape, South Africa, ²African Institute for Mathematical Sciences (AIMS), Western Cape, South Africa, ³Massachusetts General Hospital, Charlestown, Massachusetts, United States

Target Audience: This work is of interest to researchers and clinicians using functional MRI (fMRI)

Purpose: fMRI scans are typically preceded by a shimming procedure used to correct for B0 inhomogeneity (ΔB_0). This is done by acquiring a low resolution field map using, for example, a 3D gradient echo sequence. From the field map, the currents to be applied to the shim gradient coils as well as the offset in the central frequency (ΔF) are adjusted. However, fMRI is characterized by a long acquisition time during which shim fluctuations are likely to occur (e.g., due to poor initial shimming, subject respiration [1], heating induced in the shim iron by eddy currents, mechanical vibrations [2] or subject motion), which affect BOLD measures and cannot be accounted for by a single static shim. The first aim of this study was to implement a shim measurement plus correction throughout the scan in terms of zero and first order shim; this was done by repeatedly creating a 3D field map, in real time, after each fMRI measurement using a volumetric 3D EPI navigator (vNav). Secondly, we compared the results of data acquired using (A) the standard BOLD sequence that has only real time motion correction using 'PACE' [3] (BOLD) and (B) the modified vNav BOLD sequence that has both real time motion correction and shim correction (vNav-BOLD).

Methods: The interleaved multi-slice 2D gradient echo EPI fMRI sequence was modified to acquire two 3D EPI navigators with different echo times ($\Delta TE = 2.4$ ms at 3 T) and a low spatial resolution ($8 \times 8 \times 8$ mm³) immediately following each fMRI volume. Each navigator was excited with a very small flip angle of 2° to minimize the impact of signal saturation. After each fMRI measurement, a 3D field map was reconstructed on-line and the zero-order shim (ΔF) and the first-order spatial shims (linear gradients G_x, G_y and G_z) were computed. The reconstructed 3D field map from the navigator was mapped to the smaller FOV of the fMRI volume and the corresponding shim parameters for the fMRI volume were calculated. The offset of the x, y, and z shim gradient currents were then applied simultaneously in real time and the ΔF correction was implemented by recalculating the frequency and the phase of all RF pulses as well as the ADC pulses for both the navigator and the BOLD measurement. To avoid any subtle changes in the contrast of fMRI images due to small B0 fluctuations, a threshold was applied to only correct shim changes equal to or greater than 1 μ T/m. In the vNav-BOLD sequence, Prospective Acquisition CorREction (PACE) for motion was implemented using the first of each navigator pair, while the BOLD sequence used the actual fMRI images with PACE for prospective motion correction.

All scans were performed on an Allegra 3T scanner (Siemens Healthcare, Erlangen, Germany) according to approved protocols. For two adult subjects we acquired (1) high resolution T1 images as well as resting state fMRI data using (2) the standard BOLD and (3) vNav-BOLD sequences. Scans 2 and 3 were carried out twice: firstly, where a subject was instructed to remain still and, secondly, where a subject was instructed to move at certain intervals. For all scans, navigator parameters were: TR = 16.4 ms, TE₁ = 6.6 ms, TE₂ = 9 ms, 8 x 8 x 8 mm³ voxels, matrix 32 x 32 x 28 and 2 deg flip angle. Parameters for vNav-BOLD were: TR = 2000 ms plus 1150 ms for the two navigators and shim/motion correction processing, TE = 30 ms, 33 slices, matrix size 64 x 64, in-plane FOV 256 x 256 mm², slice thickness 4 mm, and 121 volumes. The TR = 3150 ms and other parameters of the BOLD acquisition were the same as for vNav-BOLD. fMRI data were processed using AFNI's afni_proc.py (first 3 time points removed; regression of WM, CSF, motion and motion derivatives; 6mm Gaussian spatial smoothing; bandpass 0.01-0.1 Hz; T1 alignment and mapping to standard MNI space). FSL's melodic (20 components) was used to perform independent component analysis (ICA) to detect resting state networks.

Results: Figure 1 shows the fluctuations in ΔB_0 in terms of zero and first order shims, calculated during the 'stationary' (Fig. 1a) and 'intentional motion' (Fig. 1b) scans for one representative subject. The root mean square of the derivative of the motion parameters (translation and rotation) are superimposed on the graphs. Figure 2 shows a comparison of two resting state networks, whose data were acquired in the absence of intentional motion, produced by ICA: the sensorimotor and visual (IC maps thresholded at $Z > 2.3$). The vNav-BOLD results show greater left-right symmetry, as well as fewer noisy clusters.

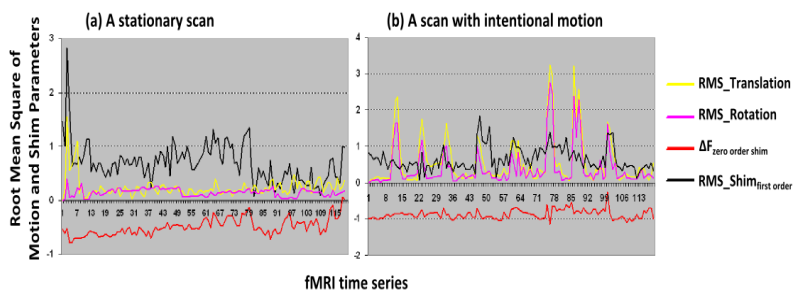


Figure 1: Derivative of the motion (translation and rotation) estimates and shim (zero and first order shim) parameters measured using vNav-BOLD during a stationary scan (a) and a scan with intentional motion (b). The units of translation in mm, rotation in degrees, first order shim μ T/m and zero order shim (ΔF) in Hz. The values of ΔF were scaled by a factor of 10 on the plots.

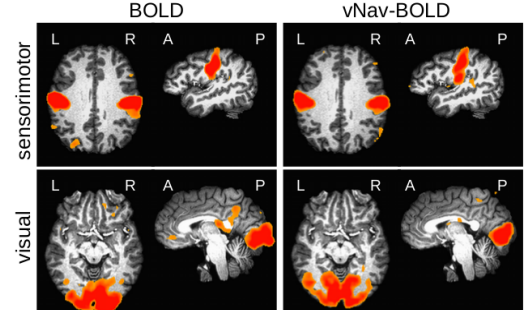


Figure 2: ICA components ($Z > 2.3$) of sensorimotor (top row) and visual (bottom row) networks, overlaid on standard space templates.

Discussion: Although both subjects were instructed to remain still during the stationary scans, incidental motion may have occurred (Fig 1a, b) and the change in ΔF and the first order shim gradients depend on the patterns of motion. In Figure 1b, although larger motion was observed at volume 78 than 48, the deviation in the shim gradients was more pronounced at volume 48, while the drift in the central frequency was larger at volume 78. The vNav-BOLD components showed greater left-right symmetry and fewer noisy clusters, likely due in part to shim corrective techniques that correct shim changes arising from incidental motion in stationary scans.

Conclusion: A major advantage of the method described here is that it can report, measure and correct simultaneously the distortion in B0 field and subject motion following each fMRI measurement. It is also worth emphasizing that the correction method is able to correct for the drift in the scanner central frequency which can be attributed to subject respiration or motion inside or outside the field of view. The proposed method will also be very efficient for high field MRI.

Acknowledgments: The South African Research Chairs Initiative of the Department of Science and Technology and National Research Foundation of South Africa, Medical Research Council of South Africa, NIH grants R21AA017410, R21MH096559, R01HD071664.

References: [1] Van de Moortele PF, Pfeuffer J, Glover GH, Ugurbil K, Hu X. Respiration-induced B0 fluctuations and their spatial distribution in the human brain at 7 Tesla. Magn Reson Med. 2002;47:888-95. [2] Benner T, van der Kouwe AJ, Kirsch JE, Sorensen AG. Real-time RF pulse adjustment for B0 drift correction. Magn Reson Med. 2006;56:204-9. [3] Thesen S, Heid O, Mueller E, Schad LR. Prospective acquisition correction for head motion with image-based tracking for real-time fMRI. Magn Reson Med. 2000;44:457-65.